Maciej WAWRZYNIAK

Poznan University of Technology, Faculty of Electronics and Telecommunications

doi:10.15199/48.2019.06.20

Effect of Nanocontacts on Transient States in Electrical Circuits

***Abstract**. This paper proposes a model of mechanical switch with stretched nanocontacts based on an analysis of the mechanisms of electron transport within a nanocontact. We use the model proposed to derive equations describing the current in a circuit with an opening switch. The measurement data and the calculation results confirm that nanocontacts substantially modify transient states in the studied circuit and therefore their effect must be taken into account in theoretical analysis.*

***Streszczenie.** W artykule na podstawie analizy mechanizmów transportu elektronów w obrębie nanozłączy zaproponowano model łącznika mechanicznego z rozciąganymi nanozłączami. Na podstawie modelu wyprowadzono wzory opisujące prąd płynący w obwodzie elektrycznym podczas otwierania łącznika. Wyniki pomiarów i obliczeń potwierdziły, że nanozłącza w sposób znaczny modyfikują stany nieustalone prądu w badanym obwodzie, co potwierdza konieczność uwzględnienia tego efektu w analizie teoretycznej. (**Wpływ nanozłączy na stany nieustalone w obwodach elektrycznych**).*

Keywords: transient states in circuits, contact resistance, nanocontacts
Słowa kluczowe: stany nieustalone w obwodach, rezystancja styku, nanozłącza

Introduction

Atomic-sized conductors have been intensively studied for more than ten years, resulting in the discovery of many interesting effects that do not occur in conductors larger in size [1]. A two-position switch [2] and a transistor [3] based on a single metal nanocontact placed on a substrate have been designed and verified to operate. Nanocontacts have been proposed to be used in sensors for the detection of lead and copper ions [4], terahertz signals [5] and linear shift [6]. Studies have also shown that nanocontacts can form between the contacts of a mechanical relay [7, 8] or a MEMS switch [9]. Of special importance is the observation of nanocontacts created in MEMS switches, used in radar components [10] and reduced power consumption systems [11]. Intensive research is conducted to improve the reliability, lifetime and switching rate of micromechanical switches. This requires an in-depth insight into the temperature effects [12], adhesion [13], creep [14] and wear [15]. The resistivity and hardness of the contact material as well as the surface topography affect the contact resistance [16]. The observed creation of nanocontacts makes this effect relevant for the analysis of the properties of MEMS switches and circuits including MEMS switches.

Using switches in an electrical circuit results in the occurrence of transient states in the circuit when a switch is being opened or closed. A switch in a circuit is modeled as a two-state device characterized by two parameters, the closed-state resistance and the open-state resistance. However, if a nanocontact forms between its terminals in the opening or closing process, a switch cannot be modeled as a two-state element. This must be taken into consideration in the analysis of transient states in an electrical circuit including such a switch, as discussed in Ref. [17] for the final stage of the opening process. In this paper we present measurements and a theoretical analysis of the whole process of opening a mechanical switch and derive equations that fully describe the current-time dependence in transient states.

Model of mechanical switch with stretched nanocontacts

When a mechanical switch is being closed its electrodes collide and a contact is made between the compressed electrodes. The compressive force acting on the electrodes is referred to as the contact force. The conductance of the contact increases with the contact force [18]. An adhesive connection is created as a result of the collision and compression of the electrodes. In an opening mechanical switch the electrodes move apart; the contact force decreases at first and then reverses direction, which results in stretching the adhesive connection area. Due to surface irregularities, a number of contact spots occur between the separating electrodes [19, 20]; these nanocontacts break successively as the electrodes continue to move apart. At the final stage of the stretching process a single nanocontact remains between the electrodes. This nanosized neck between the macroscopic electrodes narrows to the size of a single atom to break in the end [1]**.** Figure 1a shows the conductance trace (i.e., the measured time dependence of the conductance) of a contact created between the gold electrodes of an opening switch. The measurements were performed with an experimental setup described in Ref. [21].

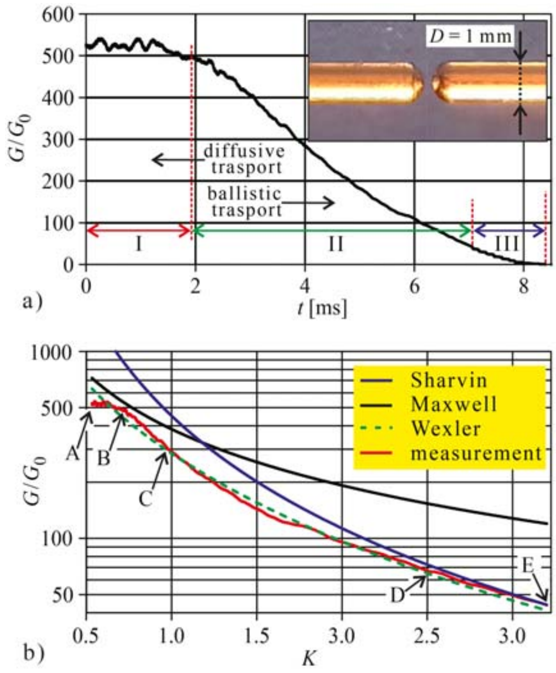

Fig.1. a) Conductance trace of the contact between the gold electrodes of an opening mechanical switch (see text for details). In the inset (top left), photograph of the electrodes of the mechanical switch used in the measurements. b) Calculated Sharvin, Maxwell and Wexler conductances vs. Knudsen number, compared with the experimental dependence resulting from the measurement data presented in a) (see text for details)

In this experiment we used a homemade switch with copper electrodes coated with a 5 μm thick nickel layer and a 0.2 μm thick gold layer on top. The switch offered a choice of electrode separation rates, which are proportional to the contact stretching rates. The photograph in Fig. 1a, inset, shows the electrodes (with diameter $D = 1$ mm) with hemispherical ends (of radius $D/2$). In the three ranges indicated in Fig. 1a the shape of the characteristic results from different mechanisms of contact stretching and electron transport in the contact. Range I, indicated with a red double-ended arrow line, corresponds to the initial phase of electrode separation. Immediately before this phase the electrodes were compressed. As the electrodes move apart, the nanocontacts between them break successively, resulting in mechanical instabilities, which can lead to a short-time increase, observed in range I, in the conductance-time dependence. Also surface contaminants have a substantial effect on the conductance of the contact in this range [22]. Indicated with a green double-ended arrow line, range II corresponds to the next phase of contact stretching. The shape of the conductance-time dependence in this range is due to the mechanism of electron transport, which changes from diffusive to ballistic with decreasing contact radius [1, 18]. In range III (blue double-ended arrow line) the conductance changes in a stepwise fashion. The conductance plateaus observed in this region correspond to metastable atom configurations in a single stretched nanocontact. In a metastable atom configuration the conductance is roughly constant and the nanocontact undergoes elastic deformation until the stress reaches a critical value and the system relaxes abruptly to another metastable configuration [23, 24]. Atom reconfigurations occur in the narrowest part of the nanocontact/neck and result in plastic deformation. Sudden reconfigurations of atoms in a stretched nanocontact following an elastic stretching phase occur also in region II. However, in this region atom reconfigurations are more frequent and the conductance plateaus corresponding to elastic stretching are poorly visible [23].

For the comparison of the measurement data obtained for regions I and II with the theoretical dependences based on the Sharvin conductance formula [25]:

$$G_S = G_0\left(\pi\frac{A}{\lambda_F^2} - 0.5\frac{P}{\lambda_F}\right), \tag{1}$$

assuming that the minimal cross section A of a nanocontact is a circle with radius r ($A = \pi r^2$, circumference $P = 2\pi r$), we determine r for a single nanocontact:

$$r = \left(1 + \sqrt{1 + 4\frac{G_S}{G_0}}\right)\frac{\lambda_F}{2\pi}, \tag{2}$$

where G is the conductance of the nanocontact, $G_0 = 2e^2/h$ the conductance quantum, and λ_F the electron Fermi wavelength (≈ 0.52 nm in gold). Next, from equation (2) we determine r for the last experimental value of G/G_0 in range II; the obtained radius is $r = 1.17$ nm. In the characteristic presented in Fig. 1a this point is just before the appearance of conductance steps. Thus, we can assume ballistic electron transport and use the Sharvin formula. We can also assume that there is only one nanocontact between the electrodes, as indicated by the conductance steps following region II. In many studies such conductance steps have been observed in a single stretched nanocontact [1].
Equation (2) can be rewritten as [26]:

$$G_S = \frac{3\pi r^2}{4\rho l}, \tag{3}$$

where ρ is the resistivity and l the electron mean free path. From equation (3) we calculate the resistivity for the value of r determined above and $l = 3.8$ nm (Ref. 24). We obtain $\rho = 2.26\cdot10^{-7}$ Ω·m, a value an order of magnitude larger than the resistivities of macroscopic conductors. The Sharvin equation can be used in the case of ballistic electron transport; in a conductor with a cross-section radius r this corresponds to $r < l$. If $r >> l$, the electron transport is diffusive, and the resistance of the conductor should be determined from the classical Maxwell formula (also known as Holm's classical relation) [26, 1, 18]:

$$G_M = \frac{2r}{\rho}. \tag{4}$$

The transition region between the diffusive and ballistic transport regimes (with $r \sim l$) is referred to as quasiballistic. The conductance in this regime can be determined from the interpolation Wexler formula [27] modified by Mikrajuddin et al. (Ref. 28):

$$G_W = \frac{G_S}{1 + \frac{G_S}{G_M}\Gamma_M(K)}, \tag{5}$$

where K is the Knudsen number ($K = l/r$). The original Wexler formula contains a slowly varying function $\Gamma(K)$, which is replaced by $\Gamma_M(K)$ in equation (5) (Ref. [28, 29]):

$$\Gamma_M(K) = \frac{2}{\pi}\int_0^\infty e^{-Kx}\operatorname{sinc}(x)dx, \tag{6}$$

For the comparison of the measurement data for ranges I and II with theoretical curves based on equations (3), (4) and (5) we assume a linear decrease of the effective contact radius from $r_{eff} = r_{max}$ to the value $r_{eff} = r_{min} = 1.17$ nm determined above; the effective contact radius r_{eff} allows for the possibility of multi-nanocontact connection between the electrodes. For the determination of r_{eff} in the contact stretching phase with more than one contact spot between the electrodes the nanocontacts can be regarded as resistors connected in parallel [30]. This, under the assumption that the cross section of each nanocontact in its narrowest point is circular, leads to the relation:

$$r_{eff} = \sqrt{\sum_i r_i^2}, \tag{7}$$

where r_i is the radius of nanocontact i. Figure 1b compares the Sharvin (blue solid line), Maxwell (black solid line) and Wexler (green dashed line) conductance values determined from equations (3), (4) and (5), respectively, with the measurement data obtained for ranges I and II. The conductance values are plotted versus the Knudsen number K in the range $K_1 = l/r_{max}$ to $K_2 = l/r_{min}$ ($r_{min} = 1.17$ nm, $l = 3.8$ nm). The assumed value of $r_{max} = 7.14$ nm provides the best fit of the experimental data to the Wexler conductance formula. Arrows in the plot indicate characteristic points A, B, C, D and E of the experimental dependence. To a good approximation, the experimental data fit the theoretical curve resulting from the Wexler formula between points C and D. Between D and E, as predicted, the experimental conductance characteristic draws near to the Sharvin dependence. Also confirming predictions, the experimental characteristic approaches the Maxwell dependence between C and B. In the segment between points B and A the experimental characteristic diverges from the Maxwell dependence. The adopted model assumes constant resistivity and mean free path in the whole range considered. A more detailed model should allow for changes of these physical quantities with the contact radius. Our model also assumes a linear time dependence of the nanocontact radius. Locally, however, r can follow a different time dependence, as a consequence of the changing (elastic, elastic-plastic and plastic) character of the contact stretching. Moreover, in the initial phase of the separation of the electrodes, when the contact force decreases, r_{eff} is directly proportional to the square root of the contact force [18, 19]. Also the effects of adhesion energy of contact surfaces, roughness and mechanical stiffness of the electrodes, surface impurity layer, temperature and humidity [31, 13, 12] could be taken into account in the model for a better fit between points B and A.

In range III the diameter of a nanocontact is comparable with the Fermi wavelength of electrons. The total conductance of a nanocontact is determined by the number of electron wave modes passing through the narrowest part of the metastable atom configuration in the nanocontact. In electrical terms, electron wave modes propagating through a nanocontact are referred to as conductance channels. Using the model of nanocontact and the method of calculating electrical conductance proposed by Rolf Landauer we obtain the following relation, which provides a basis for the determination of the conductance of a nanocontact [1]:

$$G = G_0 \sum_{n=1}^{N} T_n \ , \tag{8}$$

where $G_0 = 2e^2/h$ is the conductance quantum, T_n denotes the total transmission probability through the n-th conductance channel, and N is the number of conductance channels considered. The transmission probability can take on values in the range $0 \le T_n \le 1$. Transmission probability $T_n = 0$ means that the n-th conductance channel is closed. When $T_n = 1$, the conductance of the n-th channel is equal to the conductance quantum G_0 (which corresponds to a channel resistance of ca. 12.9 kΩ). For $0 < T_n < 1$ the conductance of the n-th channel is smaller than G_0 (the channel is only partially open, and its resistance greater than 12.9 kΩ). Conductance steps higher than G_0 (resistance < 12.9 kΩ) occur as a result of closing two or more conductance channels in the nanocontact between two successive metastable atom configurations.

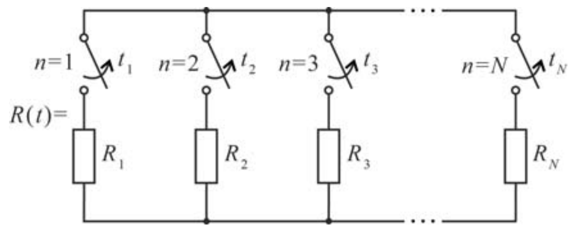

Fig. 2. Model of stretched nanocontact for range III in Fig. 1(a)

Figure 2 presents the proposed model of stretched nanocontact for range III, in which successive conductance channels close as the nanocontact is being stretched. In the diagram shown in Fig. 2 conductance channels are modeled as resistances connected in parallel. The closing of conductance channel n in the nanocontact corresponds to the opening of disconnector n. The resistance values before and after the closing of conductance channel n (the opening of switch n), denoted below by R_{n-} and R_{n+}, respectively, obey the equations:

$$R_{n-} = 1 \Big/ \sum_{k=n}^{N} \frac{1}{R_k} \quad \text{for} \quad t_{n-1} \le t < t_n \ , \tag{9}$$

$$R_{n+} = 1 \Big/ \sum_{k=n+1}^{N} \frac{1}{R_k} \quad \text{for} \quad t_n \le t < t_{n+1} \ , \tag{10}$$

where n is the channel number in order of closing ($n = 1, 2, 3, ..., N$), N is the total number of conductance channels considered, t_n the time of closing of channel n, t_0 a reference time (for $n = 1$ $t = t_0$, which corresponds to the beginning of the analysis), and R_k denotes the resistance of channel k. The resistance R_{N+} of the nanocontact after the closing of the last conductance channel fulfills the equation:

$$1/R_{N+} = 0 \quad \text{for} \quad t \ge t_N \ . \tag{11}$$

From equations (9) and (10) it follows that for n = 2, 3, ..., N:

$$R_{(n-1)+} = R_{n-} \ . \tag{12}$$

Once the resistance values before and after the closing of successive conductance channels are known, the resistances R_1, R_2, R_3, ..., R_N of the conductance channels can be determined from the following relation, resulting from equations (9) and (10):

$$R_n = \frac{R_{n-} R_{n+}}{R_{n+} - R_{n-}} \ , \tag{13}$$

where $n < N$ and $R_n = R_{n-}$ for $n = N$; resistances R_{n-} and R_{n+} are the plateau values in the conductance trace in the stepped conductance range.

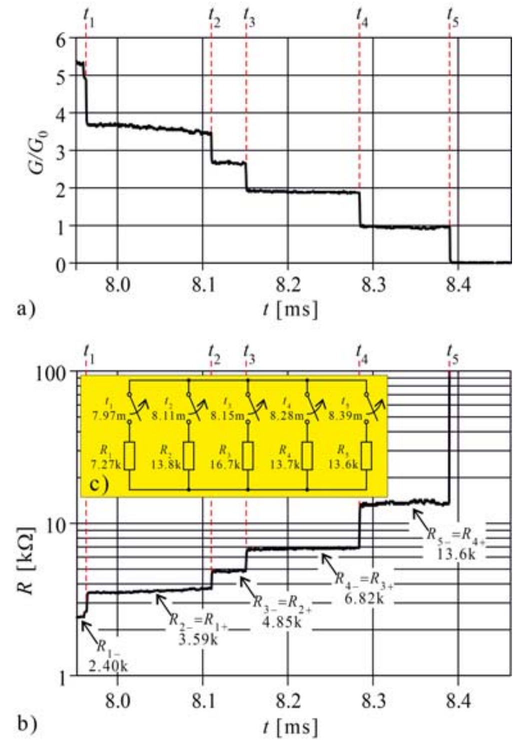

Fig. 3. Stepwise changes of the conductance and resistance of a stretched nanocontact: a) the last five conductance steps before the breaking of the nanocontact in range III in Fig. 1a; b) the corresponding time dependence of the nanocontact resistance; c) nanocontact model based on equation (12)

Figure 3a shows the last five conductance steps in range III of the conductance trace presented in Fig. 1a. The corresponding time dependence of the nanocontact resistance is shown in Fig. 3b. The number of conductance channels considered is $N = 5$. Successive channels close at times t_1, t_2, t_3, t_4 and t_5. The resistance plateau values R_{1-}, R_{2-}, R_{3-}, R_{4-} and R_{5-} are indicated by arrows in the plot. The resistance values R_1, R_2, R_3, R_4 and R_5 corresponding to the closing of successive conductance channels in the adopted model are calculated from equation (13). Figure 3c presents the model of the considered nanocontact, the conductance trace of which is shown in Fig. 3a

Comparison of theoretical and experimental results. Continuous nonocontacts conductance changes

The nanocontacts that can form between the electrodes of an opening switch have an influence on the transient states of the current in the circuit containing the switch. Because of the changing character of the conductance-time dependence in the opening switch, the current in the circuit should be analyzed first in the range preceding the conductance steps, with continuous conductance changes (ranges I and II in Fig. 1a), and only then in the stepped conductance range (range III in Fig. 1a). In the range preceding the conductance steps the current in the circuit results from the time variation of conductance due to the stretching of the contact between the electrodes. Figure 4a shows an electrical circuit represented by an impedance Z at the moment of disconnecting of a voltage V by a switch Sw. A resistance R is included in the circuit for current measurement.

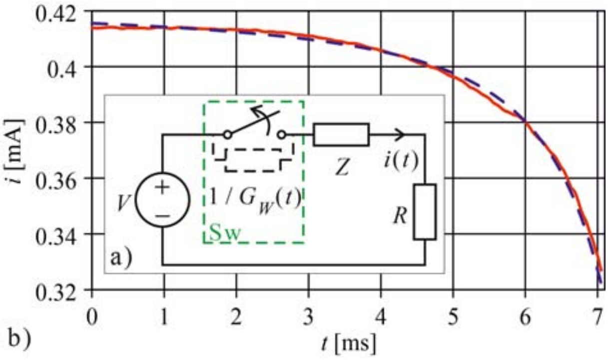

Fig. 4. Transient state in a circuit before the occurrence of conductance steps (ranges I and II in Fig. 1a): a) diagram of the circuit for the measurement of the current $i(t)$; b) the measured current (red solid line) compared with the current calculated from equation (14) (blue dashed line)

The current in the circuit in a transient state (during the opening of the switch) before the occurrence of conductance steps can be calculated from the following equation:

$$i(t) = V\left(\frac{1}{G_W(K)} + \mathrm{Re}(Z) + R\right)^{-1}, \tag{14}$$

where $G_W(K)$ can be calculated from equation (5) for $K = l/r(t)$. The time dependence of the contact radius in the model described above can be calculated from the following equation:

$$r(t) = r_{\min} + a(t_{\max} - t), \tag{15}$$

where $r_{\min}$ is the nanocontact radius calculated from equation (2) for the measurement point directly before the conductance steps (last point in range II in Fig. 1(a)), for which $t = t_{\max}$; a is the rate of change of r per unit of time resulting from the fitting of the experimental data (red solid line in Fig. 1b) to the Wexler conductance formula (green dashed line in Fig. 1b) for a given rate of electrode separation ($0.847 \cdot 10^{-6}$ m/s for the results presented in Fig. 1b). Figure 4b compares the instantaneous current measured in the range preceding the conductance steps (red solid line) with theoretical values calculated from equation (14) (blue dashed line). The good agreement between the theoretical dependence and the experimental data validates the model and the theoretical current-time dependence used.

Comparison of theoretical and experimental results. Stepped nonocontacts conductance changes

A number of successive transient states may occur in a circuit containing a mechanical switch when conductance decreases in steps as a result of nanocontact stretching. Each if these transient states is caused by the closing of a conductance channel in the stretched nanocontact. Figure 5a shows an electrical circuit represented by an impedance Z at the moment of removing a voltage V by a mechanical switch Sw in the phase where conductance decreases in steps as the nanocontact created between the contacts of the switch is being stretched.

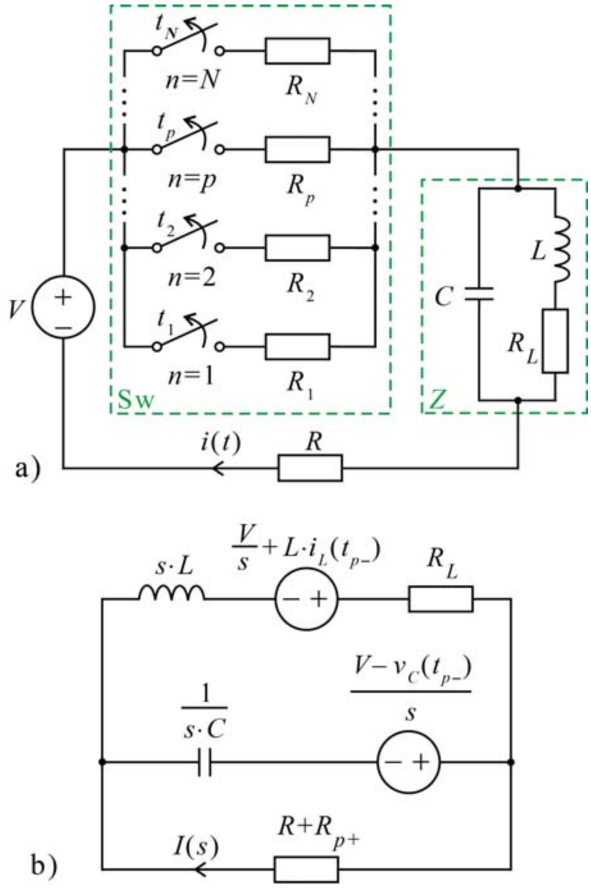

Fig. 5. Analysis of current in the circuit at the moment of opening of switch Sw in the phase where conductance decreases in steps as a result of nanocontact stretching between the terminals of the opening switch: a) diagram of the circuit used in the analysis; b) Laplace model of diagram a) after transformations

Based on the model of the nanocontact, the channel resistances R_1, R_2, ..., R_N can be determined as described in second section. Nanocontact resistances R_{p-} and R_{p+} before and after the opening of switch $n = p$ (closing of channel $n = p$), respectively, can be determined from equations (9) and (10) with $n = p$. The effect of the stepwise changes in the nanocontact conductance on the transient states of the current $i(t)$ will be the most apparent if the impedance Z of the circuit connected to the switch Sw can be replaced by the equivalent circuit, shown in Fig. 5a, with inductance L, resistance R_L, and capacitance C. Also shown in the diagram is a resistor R, included for the measurement of the current $i(t)$ in the circuit. Using this schematic we are going to determine the current $i(t)$ in the circuit after closing of channel p, which is represented by the open switch p in the diagram.

Figure 5b shows the Laplace model of the circuit presented in Fig. 5a transformed for the determination of the current $I(s)$ after the opening of switch p (where s is the Laplace operator). In this diagram the instantaneous current flowing through the inductor L immediately before the opening of switch p (at time t_{p-}) is denoted by $i_L(t_{p-})$, and the instantaneous voltage across the capacitor C immediately before the opening of switch p (at time t_{p-}) is denoted by $u_C(t_{p-})$. Using the loop current method we determine the current $I(s)$ in the circuit in the Laplace domain:

(16) $$I(s) = \frac{A_1 + A_2 s + A_3}{s\left(s^2 + A_4 s + A_5\right)}.$$

Formulas for the determination of the constants A_1 to A_5 are provided in Appendix. Next, from equation (16) we determine the inverse Laplace transform for aperiodic and periodic circuits. In an aperiodic circuit the values of R_{p+}, R, L, R_L and C must fulfill the condition:

(17) $$A_4^2 - 4A_5 > 0.$$

In this case the current $i(t)$ in the circuit has the following time dependence:

(18) $$i(t_x) = B_1 + B_2 e^{B_3 t_x} + B_4 e^{B_5 t_x},$$

where $t_x = t - t_p$, and B_1, B_2, B_3, B_4, B_5 are constants specified in the Appendix. In a periodic circuit the condition to be fulfilled by the values of R_{p+}, R, L, R_L and C is:

(19) $$A_4^2 - 4A_5 < 0.$$

In this case the current in the circuit has the time dependence:

(20) $$i(t_x) = B_1 + B_6 e^{B_7 t_x} \sin(B_8 t_x) + B_9 e^{B_7 t_x} \cos(B_8 t_x),$$

where $t_x = t - t_p$, and B_1, B_6, B_7, B_8 and B_9 are constants specified in the Appendix. Under the assumption that immediately before the opening of switch p (at time t_{p-}) the circuit was in a steady state, the instantaneous values of the current $i_L(t_{p-})$ flowing through the inductor L and the voltage $v_C(t_{p-})$ across the capacitor C can be calculated from the respective equations:

(21) $$i_L(t_{p-}) = \frac{V}{R + R_L + R_{p-}},$$

(22) $$v_C(t_{p-}) = i_L(t_{p-}) R_L.$$

If at time t_{p-} the circuit was not in a steady state, the time dependences of the current i_L and voltage v_C before opening disonector p must be determined to provide a basis for the calculation of the instantaneous values of i_L and v_C at time t_{p-}.

To verify equations (18) and (20) we simulated the impedance Z in the circuit shown in Fig. 5 by a capacitor with capacitance $C = 330$ pF and an inductor with inductance $L = 94$ mH and winding resistance $R_L = 409\ \Omega$ connected in parallel. In Fig. 6a we present the current trace measured during the opening of the switch Sw. For better readability, the graph only shows every twentieth signal sample, plotted with red diamonds. The current steps visible in the graph correspond to the last five steps in the conductance trace of the nanocontact created between the terminals of the switch. The respective times are denoted by t_1 to t_5. Next, using the method described in second section, we constructed a model of the switch based on the current-time dependence presented in Fig. 6a. The constructed model is shown in Fig. 6b.

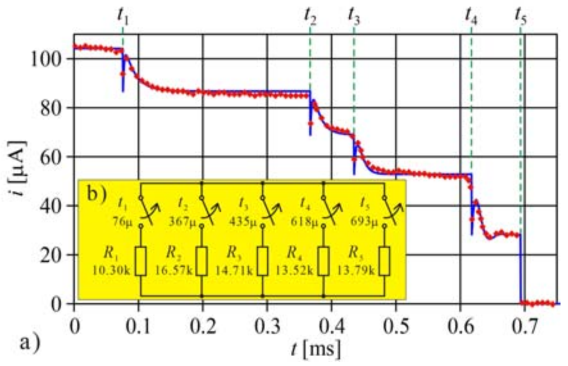

Fig. 6. a) Experimental current-time dependence (red diamonds) compared with the characteristic resulting from the theoretical analysis (blue solid line) for the case when the character of the circuit changes from aperiodic to periodic (at time t_{4+}) as a result of a stepwise decrease in conductance. b) Model of mechanical switch used in the calculations

To decide which of the above-derived equations describing the time dependence of the current in the circuit should be used for the determination of the theoretical dependence we checked the character of the circuit after the opening of each disconnector in the switch model at times t_1, t_2, t_3 and t_4. After the opening of the model disconnectors at times t_1, t_2 and t_3 the circuit parameters fulfill the inequality (17), which indicates that the circuit is aperiodic and the instantaneous current values can be calculated from equation (18). The opening of the model disconnector at time t_4 results in circuit parameters fulfilling the inequality (19); thus, the circuit has a periodic character and the instantaneous current can be calculated from equation (20). The circuit parameter values adopted for inequality testing are: $C = 330$ pF, $L = 94$ mH, $R_L = 409\ \Omega$, $R = 1\ \text{k}\Omega$, and $R_{1+} = 3.64\ \text{k}\Omega$, $R_{2+} = 4.66\ \text{k}\Omega$, $R_{3+} = 6.83\ \text{k}\Omega$, $R_{4+} = 13.79\ \text{k}\Omega$. In the next step we determined analytically the instantaneous current, using equation (21) for the range $0_+ \le t \le t_{1-}$, equation (18) for $t_{1+} \le t \le t_{2-}$, $t_{2+} \le t \le t_{3-}$, $t_{3+} \le t \le t_{4-}$, and equation (20) for $t_{4+} \le t \le t_{5-}$. For times $t \ge t_{5+}$ the current in the circuit is 0. The analytical current-time dependence is represented by the blue solid line in the plot shown in Fig. 6a.

Since the resistance of a switch with a nanocontact increases in time as successive disconnectors open in the model circuit, there are three possible scenarios of changes in character of the circuit as a result of the stretching of the nanocontact: the circuit is aperiodic after each conductance step, the circuit changes from aperiodic to periodic (case illustrated by Fig. 6), or the circuit is periodic after each conductance step. The latter case is illustrated by Fig. 7a, showing four current steps at times t_1, t_2, t_3 and t_4 measured in the circuit presented in Fig. 5a with the following parameters: $C = 948$ pF, $L = 7.05$ mH, $R_L = 168\ \Omega$, $R = 1\ \text{k}\Omega$. For better readability, the plot only includes every twentieth sample of the measured characteristic (red diamonds). The experimental data are compared with the characteristic determined analytically (blue solid line).

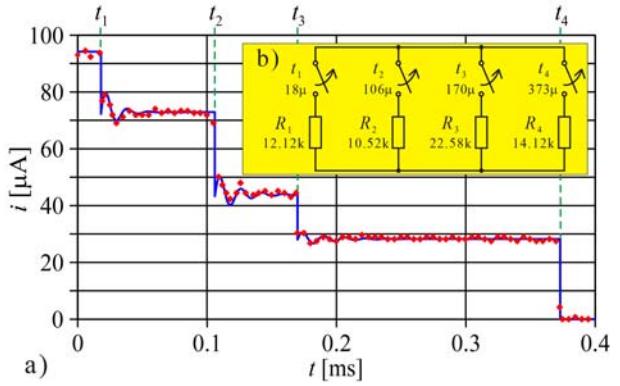

Fig. 7. a) Experimental current-time dependence (red diamonds) compared with theoretical characteristic (blue solid line) for the case when the circuit is periodic after the current steps. b) Model of mechanical switch used in the calculations

Figure 7b shows the model of the switch used in the analysis. The instantaneous current is determined from equation (21) for the range $0_+ \le t \le t_{1-}$, and from equation (20) for $t_{1+} \le t \le t_{2-}$, $t_{2+} \le t \le t_{3-}$, and $t_{3+} \le t \le t_{4-}$. After the opening of the model disconnectors at times t_1, t_2 and t_3 the circuit parameters fulfill the inequality (19), which means that the circuit is periodic. Besides the parameters specified above, we put $R_{1+} = 4.758$ kΩ, $R_{2+} = 8.689$ kΩ and $R_{3+} = 14.123$ kΩ. for inequality testing. For times $t \ge t_{5+}$ the current in the circuit is 0.

Figures 6a and 7a indicate that the current traces determined analytically are in good agreement with the experimental data, which validates the model proposed and the theoretical current-time dependences derived.

Summary

Our study and the analysis of its results demonstrate that when nanocontacts form between the terminals of an opening switch, its contact resistance results from the conductance of the stretched nanocontacts. The experimentally determined time dependence of the conductance of the switch used in the study has two segments that differ in the character of conductance changes, continuous in one segment and stepwise in the other. In the first segment the conductance of the opening switch can be determined based on the Wexler model, as described in the second section. In the other segment the conductance steps have a stochastic character and the conductance can be described by the Landauer formula. This equation provides a basis for the proposed model, with conductance channels represented by resistors connected in parallel. The resistances of the model resistors can be determined from the measured stepped conductance trace.

Using the adopted models, we have determined the theoretical time dependences of the current in the circuit during the opening of the switch. For verification of the theoretical dependence we have measured the current at the time of opening of a mechanical switch removing voltage from a circuit represented by impedance Z. The measurement data, in good agreement with the calculation results, show that nanocontacts created between the terminals of an opening mechanical switch modify the transient states of the current in a circuit connected with the switch. This effect must be taken into account in the analysis of transient states in electrical circuits.

In the initial phase of switch opening the current-time dependence can be determined analytically from an equation derived from the Wexler conductance formula. An especially interesting phenomenon is observed at the time of closing of conductance channels just before the last nanocontact breaks. Short-lived transient states occur in this phase as a result of the closing of successive conductance channels. For the determination of the current-time dependence in this final phase of switch opening the character of the circuit, which can be aperiodic or periodic, should be tested for an appropriate choice of theoretical equation.

Appendix

The constants in formulas (16), (17) and (19) can be determined from equations (23) to (27).

(23) $$A_1 = b_4 - b_{10}$$

(24) $$A_2 = (b_4 - b_{10})b_1 - b_6$$

(25) $$A_3 = b_9 b_4$$

(26) $$A_4 = b_2$$

(27) $$A_5 = 0.25 b_3$$

The constants in equations (18) and (20) can be determined from equations (28) to (36).

(28) $$B_1 = b_5$$

(29) $$B_2 = \frac{b_4 - b_{10} - b_5}{2} + \frac{(b_4 - b_{10})b_1 + b_6 - 0.5(b_4 - b_{10} + b_5)b_2}{b_7}$$

(30) $$B_3 = -0.5(b_2 - b_7)$$

(31) $$B_4 = \frac{b_4 - b_{10} - b_5}{2} + \frac{0.5(b_5 + b_4 - b_{10})b_2 - (b_4 - b_{10})b_1 - b_6}{b_7}$$

(32) $$B_5 = -0.5(b_2 + b_7)$$

(33) $$B_6 = \frac{b_6 + (b_4 - b_{10})b_1 - b_2\left[b_5 + 0.5(b_4 - b_{10} - b_5)\right]}{0.5 b_8}$$

(34) $$B_7 = -0.5 b_2$$

(35) $$B_8 = 0.5 b_8$$

(36) $$B_9 = b_4 - b_{10} - b_5$$

The auxiliary constants in equations (23) to (36) can be determined from equations (37) to (46).

(37) $$b_1 = \frac{R_L}{L}$$

(38) $$b_2 = b_1 + \frac{1}{(R + R_{p+})C}$$

(39) $$b_3 = 4\frac{R_L + R + R_{p+}}{(R + R_{p+})LC}$$

(40) $$b_4 = \frac{V}{R + R_{p+}}$$

(41) $$b_5 = \frac{V}{R_L + R + R_{p+}}$$

(42) $$b_6 = \frac{i_L(t_{p-})}{(R + R_{p+})C}$$

(43) $$b_7 = \sqrt{b_2^2 - b_3}$$

(44) $$b_8 = \sqrt{b_3 - b_2^2}$$

(45) $$b_9 = \frac{1}{LC}$$

(46) $$b_{10} = \frac{v_C\left(t_{p-}\right)}{R + R_{p+}}$$

Acknowledgement
The present study has been funded by the Polish Ministry of Science and Higher Education within the statutory activity, task 08/83/DSPB/4727 in 2018.

***Author**: dr hab. inż. Maciej Wawrzyniak, Poznań University of Technology, Faculty of Electronics and Telecommunications, Piotrowo 3A, 60-965 Poznań,*
E-mail: maciej.wawrzyniak@put.poznan.pl

REFERENCES

[1] Agraït N., Yeyati A. L., Van Ruitenbeek J. M., Quantum properties of atomic-sized conductors, *Physics Reports*, 377 (2003), 81-279.

[2] Terabe K., Hasegawa T., Nakayama T., Aono M., Quantized conductance atomic switch, *Nature*, 433 (2005), 47-50.

[3] Xie F., Maul R., Obermair C., Wenzel W., Schön G., Schimmel T., Multilevel atomic-scale transistors based on metallic quantum point contacts, *Advanced Materials*, 22 (2010), 2033-2036.

[4] Rajagopalan V., Boussaad S., Tao N. J., Detection of heavy metal ions based on quantum point contacts, *Nano Letters*, 3 (2003), 851-855.

[5] Song J., Aizin G., Kawano Y., Ishibashi K., Aoki N., Ochiai Y., Reno J. L., Bird J. P., Evaluating the performance of quantum point contacts as nanoscale terahertz sensors, *Optics Express*, 18 (2010), 4609-4614.

[6] Cleland A. N., Aldridge J. S., Driscoll D. C., Gossard A. C., Nanomechanical displacement sensing using a quantum point contact, *Appl. Phys. Lett.*, 81 (2002), 1699-1701.

[7] Hansen K., Lægsgaard E., Stensgaard I., Besenbacher F., Quantized conductance in relays, *Phys. Rev. B*, 56 (1997), 2208-2220.

[8] Yasuda H., Sakai A., Conductance of atomic-scale gold contacts under high-bias voltages, *Phys. Rev. B*, 56 (1997), 1069-1071.

[9] Poulain C., Jourdan G., Peschot A., Mandrillon V. Contact conductance quantization in a MEMS switch, *In 2010 Proceedings of the 56th IEEE Holm Conference on Electrical Contacts*, (2010).

[10] Van Caekenberghe K., RF MEMS on the radar. *IEEE Microwave Magazine*, 10 (2009), 99-116.

[11] Rebeiz G. M., Muldavin J. B., RF MEMS Switches and Switch Circuits, *IEEE Microwave Magazine*, 2 (2006), 59-71.

[12] Brown C., Rezvanian O., Zikry M. A., Krim J., Temperature dependence of asperity contact and contact resistance in gold RF MEMS switches, *Journal of Micromechanics and Microengineering*, 19 (2009), 025006.

[13] Jensen B. D., Huang K., Chow L. L. W., Kurabayashi K., Adhesion effects on contact opening dynamics in micromachined switches, *Journal of Applied Physics*, 97 (2005), 103535.

[14] Gregori G., Clarke D. R., The interrelation between adhesion, contact creep, and roughness on the life of gold contacts in radiofrequency microswitches, *Journal of Applied Physics*, 100 (2006), 094904.

[15] Patton S. T., Zabinski J. S., Fundamental studies of Au contacts in MEMS RF switches, *Tribology Letters*, 18 (2005), 215-230.

[16] Yang Z., Lichtenwalner D. J., Morris A. S., Krim, J., Kingon A. I., Comparison of Au and Au–Ni alloys as contact materials for MEMS switches, *Journal of Microelectromechanical Systems*, 18 (2009), 287-295.

[17] Nawrocki W., Wawrzyniak M., Pajakowski J., Transient states in electrical circuits with a nanowire, *Journal of Nanoscience and Nanotechnology*, 9 (2009), 1350-1353.

[18] Toler B. F., Coutu Jr R. A., McBride J. W., A review of micro-contact physics for microelectromechanical systems (MEMS) metal contact switches, *Journal of Micromechanics and Microengineering*, 23 (2013), 103001.

[19] Pal J., Zhu Y., Dao D., Lu J., Khan, F., Study on contact resistance in single-contact and multi-contact MEMS switches. *Microelectronic Engineering*, 135 (2015), 13-16.

[20] Rezvanian O., Zikry M. A., Brown C., Krim, J., Surface roughness, asperity contact and gold RF MEMS switch behavior. *Journal of Micromechanics and Microengineering*, 17 (2007), 2006-2015.

[21] Wawrzyniak M., Probe capacitance-dependent systematic error in IV measurements of nanowires: analysis and correction, *Metrology and Measurement Systems*, 14 (2007), 391-408.

[22] Dickrell D. J., Dugger M. T., Electrical contact resistance degradation of a hot-switched simulated metal MEMS contact, *IEEE Transactions on Components and Packaging Technologies*, 30 (2007), 75-80.

[23] Untiedt C., Rubio G., Vieira S., Agraït N., Fabrication and characterization of metallic nanowires, *Physical Review B*, 56 (1997), 2154-2160.

[24] Torres J. A., Sáenz J. J., Conductance and mechanical properties of atomic-size metallic contacts: a simple model. *Physical Review Letters*, 77 (1996), 2245-2248.

[25] Garcia-Martin A., Torres J. A., Sáenz J. J., Finite size corrections to the conductance of ballistic wires, *Physical Review B*, 54 (1997), 13448-13451.

[26] Erts, D., Olin, H., Ryen, L., Olsson, E., Thölén, A., Maxwell and Sharvin conductance in gold point contacts investigated using TEM-STM, *Physical Review B*, 61 (2000), 12725-12727.

[27] Wexler G., The size effect and the non-local Boltzmann transport equation in orifice and disk geometry, *Proceedings of the Physical Society*, 89 (1966), 927-941.

[28] Mikrajuddin A., Shi F. G., Kim H. K., Okuyama K., Size-dependent electrical constriction resistance for contacts of arbitrary size: from Sharvin to Holm limits, *Materials Science in Semiconductor Processing*, 2 (1999), 321-327.

[29] Coutu R. A., Kladitis P. E., Cortez R., Strawser R. E., Crane R. L., Micro-switches with sputtered Au, AuPd, Au-on-AuPt, and AuPtCu alloy electric contacts, *IEEE Trans. Comp. Pack. Tech.*, 29 (2006), 341-349.

[30] Majumder S., McGruer N. E., Adams G. G., Zavracky P. M., Morrison R. H., Krim, J., Study of contacts in an electrostatically actuated microswitch, *Sensors and Actuators A: Physical*, 93 (2001), 19-26.

[31] Broue A., Fourcade T., Dhennin J., Courtade F., Charvet P. L., Pons P., Plana R., Validation of bending tests by nanoindentation for micro-contact analysis of MEMS switches, *Journal of Micromechanics and Microengineering*, 20 (2010), 085025.